ALLEN INSTITUTE for BRAIN SCIENCE

Aging, Dementia and TBI Study

TECHNICAL WHITE PAPER:
QUANTITATIVE DATA GENERATION

OVERVIEW

This Technical White Paper describes the quantitative data components of this study, which was designed to identify long-term neuropathological and molecular consequences of mild to moderate Traumatic Brain Injury (TBI) in a large, well characterized aged cohort. These quantitative assays include:

- Transcriptome analysis of selected brain regions using RNA-Sequencing
- Quantitative neuropathology using automated image analysis of markers of degenerative pathology
- Protein measurements of disease pathology and inflammation using a Luminex platform
- Measurement of oxidative stress using isoprostane quantification

Transcriptome-wide methods (*i.e.*, microarrays and RNA-Seq) have been used to generate a comprehensive view of neurotypical gene expression signatures in the developing and adult human brain[1-6] and have also provided valuable insight into how these gene expression signatures change with disease. For example, massive gene expression changes have been seen for neurodegenerative diseases such as Alzheimer's disease and Parkinson's disease, which share many of the pathological inclusions that are seen in chronic traumatic encephalopathy (CTE)[7-9]. A primary goal of this study was to understand whether detectable changes in gene expression were correlated with exposure to TBI and/or associated neuropathologies.

In addition to transcriptome analysis, the deposition of neuropathologically associated proteins, including β-amyloid, tau, and α-synuclein were measured using several strategies. Pathology in both fixed and fresh frozen tissue was measured with immunohistochemistry and quantified using automated image analysis to generate proxy values for the severity of pathology. Protein molecular changes in tau and phospho-tau variants, Aβ species, α-synuclein, inflammatory mediators (cytokines and chemokines), neurotrophic factors, and other targets were determined using multiplexed Luminex assays complemented with traditional antibody-based methods in immediately adjacent frozen tissues from each region. Finally, measurements of free radical injury were made using gas chromatography mass spectrometry (GC/MS) quantitation of isoprostanoids in immediately adjacent frozen tissues.

All of these quantitative metrics were generated on matched samples, allowing correlations to be made between clinical, neuropathological and molecular endpoints and measurements as a means to understand the long term pathological effects and pathophysiology of neurodegeneration related to aging, dementia and TBI.

RNA SEQUENCING

Sample Collection by Macrodissection

The transcriptome was analyzed in four regions: neocortex from the posterior superior temporal gyrus and the inferior parietal lobule, white matter underlying the parietal neocortex, and the hippocampus. Because CTE-associated pathology has been identified as occurring at the depths of the sulci, cortical samples were taken from the portion of the bank of the gyrus close to the depth of the sulcus when possible. White matter samples

were taken from tissue situated close to, or beneath, the parietal cortex sample when possible. Hippocampus was sampled in its entirety, including portions of the subicular cortex.

Collection of tissue samples from temporal and parietal neocortex, hippocampus, and parietal white matter was done by manual macrodissection. Specific areas for macrodissection were first identified by neuroanatomists using images of Nissl-stained tissue sections immediately adjacent to the sampled tissue. **Figure 1** shows an annotated Nissl section with outlined macrodissection sample sites. Sample collection was therefore unbiased with respect to the presence or absence of amyloid plaques, tau deposits, or Lewy bodies. Macrodissection sites were placed to avoid tangential cuts through the cortex to control the proportional of cell types across cortical samples as much as possible; white matter was required to be visible below the sample site to ensure that the entire depth of the cortex was sampled.

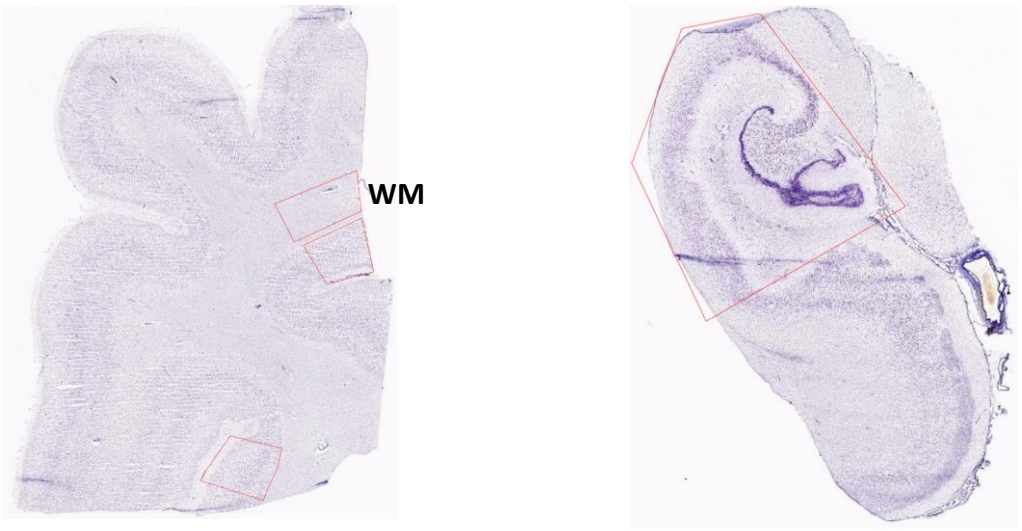

Figure 1. Example macrodissection sites for RNA isolation.
The left panel shows example macrodissection sites for parietal cortex (two gray matter sites and one white matter site (indicated by WM)). Cortical samples were taken from the portion of the bank of the gyrus close to the depth of the sulcus when possible. White matter samples were taken from tissue situated close to, or beneath, the parietal cortex sample when possible. The right panel shows an example of a hippocampal macrodissection site. The hippocampus was sampled in its entirety, including portions of the subicular cortex.

RNA Isolation for Sequencing

Tissue was kept frozen throughout the macrodissection process using a temperature-controlled dissection table maintained at -15°C. All instruments and cutting surfaces were cleaned with 70% ethanol and RNaseZAP (Applied Biosystems/Ambion, Austin, TX) and were chilled to -15°C before use. Using the annotated Nissl-stained section as a guide, the indicated areas of tissue for collection were excised from the remaining tissue (approximately 1-2 mm) of the appropriate frozen tissue block using a scalpel. Between 10–750 mg of tissue was excised during macrodissection depending on the tissue block, with an average of 95 mg across all 397 samples that were sent for sequencing (**Table 1**).

Table 1. Macrodissection information for each brain region.

Region	Range mg tissue	Average mg tissue	Number of samples	RIN
Hippocampus	20-250 mg	227 mg	103	6.3 +/- 1.1
Parietal cortex	10-130 mg	52 mg	94	6.2 +/- 1.4
Temporal cortex	10-230 mg	60 mg	106	6.5 +/- 1.2
White matter*	10-80 mg	34 mg	94	6.4 +/- 1.2

*White matter was sampled from parietal cortex.
Abbreviations: RIN, RNA Integrity Number

After dissection, each sample was immediately transferred using chilled forceps to an individual pre-weighed tube that was pre-chilled on dry ice. Care was taken to avoid unnecessary warming of the tissue or collection tube throughout the process. All surfaces and instruments were cleaned between dissections to prevent cross contamination. Tubes containing tissue were stored at -80°C until processing for RNA isolation. Nissl images with macrodissection sites are stored in a database and available online.

RNA was isolated using the RNeasy Lipid Tissue Mini Kit (Qiagen #78404) as per manufacturer's instructions. Tubes containing tissue were kept on dry ice and weighed to determine the mass of the dissected tissue. QIAZOL lysis buffer was added to achieve a 50 mg/ml concentration, with at least 1 ml of QIAZOL added for tissue samples under 50 mg. Up to 6 samples were lysed and homogenized at a time, using an Omni-Prep Homogenizer (Omni International, Kennesaw, GA). Tissue was lysed and homogenized for 1 – 2 min at 20,000 rpm. Once complete lysis was confirmed by visual inspection, tubes were incubated for 30 min in a 25°C water bath. Following incubation, samples were phase separated to isolate RNA or were stored at -80°C.

Phase separation was performed in batches of up to 24 tubes. First, 500 µl of homogenized QIAZOL lysate was added to labeled 1.5 ml tubes containing 50 µl of bromochloropropane (BCP). The contents were mixed by vortexing at maximum for 10-15 seconds, allowed to sit at room temperature for 5 minutes, and phase separated by centrifugation at 13,000 x *g* at 4°C for 15 minutes. Upper aqueous phase (230µl) was transferred to a new tube for RNA isolation following manufacturer's instructions. RNA was eluted using 30µl of RNase-free water supplied by Qiagen. The remaining QIAZOL lysate that was not phase separated was stored at -80°C in bar-coded 2 ml tubes for future use.

Two µl of eluted RNA were removed and aliquoted into a 96-well PCR plate for quantification on a Nanodrop 8000 spectrophotometer (Thermo Scientific, Wilmington, DE). Samples were then normalized to 5ng/µl before RNA QC was performed using a Bioanalyzer (Agilent Technologies) with 1µl of each 5ng/µl RNA sample loaded onto a Pico Chip. Sample electropherograms were assessed and RNA Integrity Number (RIN) was recorded. All samples, regardless of RNA quality, were sent for sequencing. RNA samples were stored at -80C until shipment for RNA Sequencing.

The average RNA Integrity Number (RIN) of all 397 samples that were sent for sequencing was 6.3, including 22 with RIN<4 and an additional 26 with 4<RIN<5 (see **Table 1**). After correcting for RNA quality in the normalization (discussed below) samples showing all levels of RNA quality, including when the Bioanalyzer traces showed degraded 18S and 28S bands, were retained in the final data set.

RNA-Seq

Total RNA (250ng) was used as input into the Illumina TruSeq Stranded Total RNA Sample Prep Kit (RS-122-2203), which uses random hexamer first strand cDNA synthesis and includes rRNA depletion (Ribo-Zero Gold rRNA depletion kit to remove both cytoplasmic and mitochondrial rRNA) and fragmentation. At the time of project inception, this sequencing strategy provided the most reliable option for quantification of transcriptomic reads from tissue of widely varying quality, allowing the broadest inclusion of donors from the ACT cohort.

ERCCs (External RNA Controls Consortium)[10,11] at a 1:10,000 dilution were spiked into each sample. A ratio of 4µl of 1:10,000 dilution was added to every 10µl of sample, for a final volume of 14µl, of which 10µl (at 25ng/µl RNA) was used as input into the TruSeq library prep. Typical working volumes were 6.9µl of ERCC (1:10,000) in 24µl total volume or 13.8µl ERCC (1:10,000) into 48µl total volume where the final RNA concentration was 25ng/µl. The first three RNA-Seq batches, however, had approximately 2-3x less ERCC added (4µl in both 24µl and 48µl total). This did not affect the sample RNA sequence data quality and to be able to assign approximate number of molecules corresponding to each FPKM (fragments per kilobase million) value and to determine a lower limit of reliable detection. RNA sequencing was done on Illumina HighSeq 2500 using v4 chemistry, producing a minimum of 30M 50bp paired-end clusters per sample. Expression Analysis, Inc. (Morrisville, NC) performed both the TruSeq Stranded Sample Prep as well as the Illumina sequencing.

RNA-Seq Data Alignment

Raw read (fastq) files were aligned to the GRCh38.p2 human genome (current as of 01/15/2016) after removing duplicate gene entries from the gff3 reference file for consistency with the Allen Institute Laboratory Information Management System (LIMS). For alignment, Illumina sequencing adapters were clipped from the reads using the fastqMCF program[12]. After clipping, the paired-end reads were mapped using RNA-Seq by Expectation-Maximization (RSEM)[13] using default settings except for two mismatch parameters: bowtie-e (set to 500) and bowtie-m (set to 100). RSEM aligns reads to known isoforms and then calculates gene expression as the sum of isoform expression for a given gene, assigning ambiguous reads to multiple isoforms using a maximum likelihood statistical model. Reads that did not map to the transcriptome were then aligned to the hg38 genome sequence using Bowtie with default settings[14]. Reads that mapped to neither the transcriptome with RSEM nor to the genome with Bowtie were mapped against the ERCC sequences. These alignment steps produce gene- and isoform-level quantifications of the transcriptome-mapped reads in several formats—raw read counts, as well as transcripts per million (TPM) and fragments per kilobase per million (FPKM), which both normalize for gene length and for the total number of reads in slightly different ways. Additional output includes chromosome-wide counts for the genomic-mapped reads, BAM files containing both transcriptome- and genome-mapped reads, and fastq files for the unmapped reads. Anonymized BAM files (where sequence-level information has been removed) and gene-level quantification (TPM, FPKM, and number of reads) are available as part of the resource (see Download tab).

RNA-Seq Data Normalization

Prior RNA-Seq analysis of different human brain regions showed minimal evidence of process batch effects, but that improvements in variability could be made after data normalization[15]. We applied a comparable post-hoc data normalization strategy, with the addition of a step to control for RNA quality which was quite variable across the sample cohort. Specifically, FPKM gene quantifications for all RNA-Seq samples were first collated from the RSEM alignments into a single data matrix. Second, this FPKM data matrix was further adjusted for the total transcript count using TbT normalization[16], which scales each sample based on the summed expression of all genes that are not differentially expressed. FPKM values were TbT normalized in linear space, with the differential expression vector was defined as TRUE if a sample was from either temporal or parietal cortex and FALSE if it is from white matter or hippocampus. Sample data was then scaled such that the total log2(FPKM) across the entire data set remained unchanged after normalization. The result of this step was that expression levels for all genes in a particular sample were multiplied by a scalar value close to 1 (in most cases between 0.9-1.2). Finally, quantifications of each gene are corrected for RNA quality independently by modeling RIN as a quadratic variable and batch as a factor variable, taking the sum of the residual and the mean as the normalized value, and then setting any negative values to 0. The following R function was used to do this step:

```
getPolyResidualsForRINandBatch <- function(TbTnormDat,RIN,batch,N=2) {
 lmOutput = lm(x ~ poly(RIN, N, raw=TRUE) + batch);
 return(pmax(mean(x) + x - predict(lmOutput),0));
}
```

where TbTnormDat is the TbT-normalized FPKM values for a given gene. This RIN and batch correction step was performed independently for each brain region, as RNA quality varied between brain regions (see **Table 1**), and many analyses will be performed on one brain region at a time.

All sequencing data underwent a quality control assessment, both before and after normalization, which included clustering samples using all genes. Ten of the samples sequenced early in the project were biological replicates (*i.e.*, run on the same brain region and donor as a previously run sample). Replicate samples showed highly consistent expression patterns and therefore only a single sample per brain region and donor are included in the final resource. An additional 10 samples (including all four samples from donor H15.09.105) had gene expression patterns highly inconsistent with other samples collected from the same brain region, suggesting that these samples do not accurately represent the tissue indicated. These samples were removed as fails, and the normalization process above was repeated. The resulting normalized data matrix of 377 samples is used in the web resource, and is also available for direct download. Several additional normalization strategies were performed on these RNA-Seq data for comparison, but none showed improvements in data quality over the method described above by any of the metrics used for comparison.

Image Analysis and Pathology Metrics

Fresh Frozen Tissue

Image analysis was performed on images acquired from immunohistochemistry (IHC) stained tissue sections (see **Table 2** for list of antibodies and associated proteins) from all tissue blocks that generated samples for RNA-Seq. All available images from a given stain were evaluated. To generate quantitative image metrics, the macrodissection sites as delineated on the Nissl images were used to guide the identification and annotation of equitable regions of interest (ROIs) on each of the near-adjacent IHC images. The ROI was adjusted if there were technical artifacts present in the desired area that would affect the evaluation of pathology. These artifacts included torn or folded tissue, air bubbles caught under the coverslip, or dust on the slide. Blood vessels that contained non-specific binding were also excluded when possible, though if they contained true staining, they were included in the ROI. If these technical artifacts could not be excluded from the ROI, it was shifted to an area with comparable staining or removed entirely.

Table 2. Antibodies and associated proteins detected in fresh frozen tissue.

Antibody	Protein	Associated Pathologies
Ab6E10	β-amyloid	Amyloid plaques, amyloid angiopathy
AT8	pS202/pT205 Tau	Pre-tangles, tangles, dystrophic neurites, astrocytic plaques, etc.
LB509	Phospho-α-synuclein	Lewy bodies, Lewy neurites

The expression density, defined as the percentage of area within the ROI that was occupied by the IHC reaction product, was then assessed algorithmically. The algorithm uses an adaptive detection/segmentation technique to generate a mask highlighting areas of enriched expression in each image (see the Expression Detection Module section in the Informatics Data Processing paper in the Allen Mouse Brain Atlas Documentation tab for more details). For each ROI, a measure of immunoreactivity was obtained by dividing the number of highlighted pixels in the mask by the total number of pixels in the ROI. Finally, for each tissue block and structure (parietal cortex, white matter underlying parietal cortex, temporal cortex, and hippocampus), a value was obtained by adding the corresponding ROI values.

Formalin-Fixed Tissue

The expression density was also assessed in IHC images obtained from slides from formalin-fixed tissue in a similar manner, the main difference being that these tissue blocks were not used to generate RNA-Seq data, and therefore there was no macrodissection site to reference. ROIs for image analysis were instead selected on images of IBA1 stained tissue, with the intent of selecting regions that represented tissue at the base of the gyrus whenever possible, using the same criteria as what was used for determining macrodissection sites on fresh frozen tissue. The IBA1 stain typically showed little variability within a given section, and was therefore chosen as a means to select ROIs independently of the presence of the various pathologies. From neocortical blocks, two ROIs for each structure were delineated, after which the same area was selected for ROI analysis on the remaining IHC-stained sections (see **Table 3**). For hippocampus, a single outline was applied that corresponded to all of Ammon's horn and the underlying subicular cortex The ROI was adjusted if there were technical artifacts present in the desired area that would affect the evaluation of pathology. These artifacts included torn or folded tissue, air bubbles caught under the coverslip, or dust on the slide. Blood vessels that contained non-specific binding were also excluded when possible, though if they contained true staining, they were included in the ROI. If these technical artifacts could not be excluded from the ROI, the ROI was shifted to an area with comparable staining or removed entirely.

Table 3. Antibodies and associated proteins detected in fixed tissue.

Antibody	Protein	Associated Pathologies
AT8	pS202/pT205 Tau	Pre-tangles, neurofibrillary tangles, dystrophic neurites, astrocytic plaques, etc.
Tau2	Hyperphosphorylated Tau	Mature neurofibrillary tangles and dystrophic neurites
Ab6E10	β-amyloid	Amyloid plaques, amyloid angiopathy
LB509	Phospho-α-synuclein	Lewy bodies, Lewy neurites
pTDP43	Phosphorylated 43-kDaTAR DNA-binding protein	Cytoplasmic inclusions consisting of phosphorylated TDP43
GFAP	Glial fibrillary acidic protein	Astrocytes
IBA1	Ionized calcium binding adapter molecule 1	Microglia

As in the case of fresh frozen tissue, an expression density value was calculated for each structure in each tissue block. In contrast to the fresh frozen tissue, however, the expression masks were calculated only after applying a spectral filter that attenuated the signal from the hematoxylin stained nuclei and the Luxol Fast Blue stained fibers.

Analysis of Expression Density

All expression density values were assessed for each region and across each stain. For stains with very low expression densities, ROIs that were identified as outliers were visually inspected to determine if the values represented the presence of actual pathology or whether high values resulted from technical artifacts. Those that resulted from artifacts were then adjusted or removed as necessary. The resulting expression density values were averaged across all ROIs for a given donor, structure, and stain combination, providing a single data point for each combination.

To validate the metrics that were generated, antibodies that were used on both the fresh frozen and formalin fixed sections were correlated. Although blocks of tissue were from the same brain region, section thickness and methodologies differed significantly between tissue types, and hippocampal fixed and frozen tissues came from opposite hemispheres. Despite those caveats, good correlations were seen between the antibodies for Aβ and AT8 (**Figure 2**), and the distribution of values was remarkably similar, suggesting that staining was comparable across the different fixation conditions, and that comparable masks were being generated for both tissue conditions. In contrast, α-synuclein stain quantification differed between methods, most notably showing a discrepancy in the distribution of values between the staining for fresh frozen and formalin fixed tissue resulting in low correlation. Upon review of the data, the more Gaussian distribution of data points for the formalin-fixed tissue resulted from poor discrimination of signal and noise in cases with no pathology, which constituted the vast majority of tissue blocks. The image analysis data for the α-synuclein stain is only provided for the fresh-frozen tissue as the expression quantification for the FFPE treated tissue was found to have low signal to noise values.

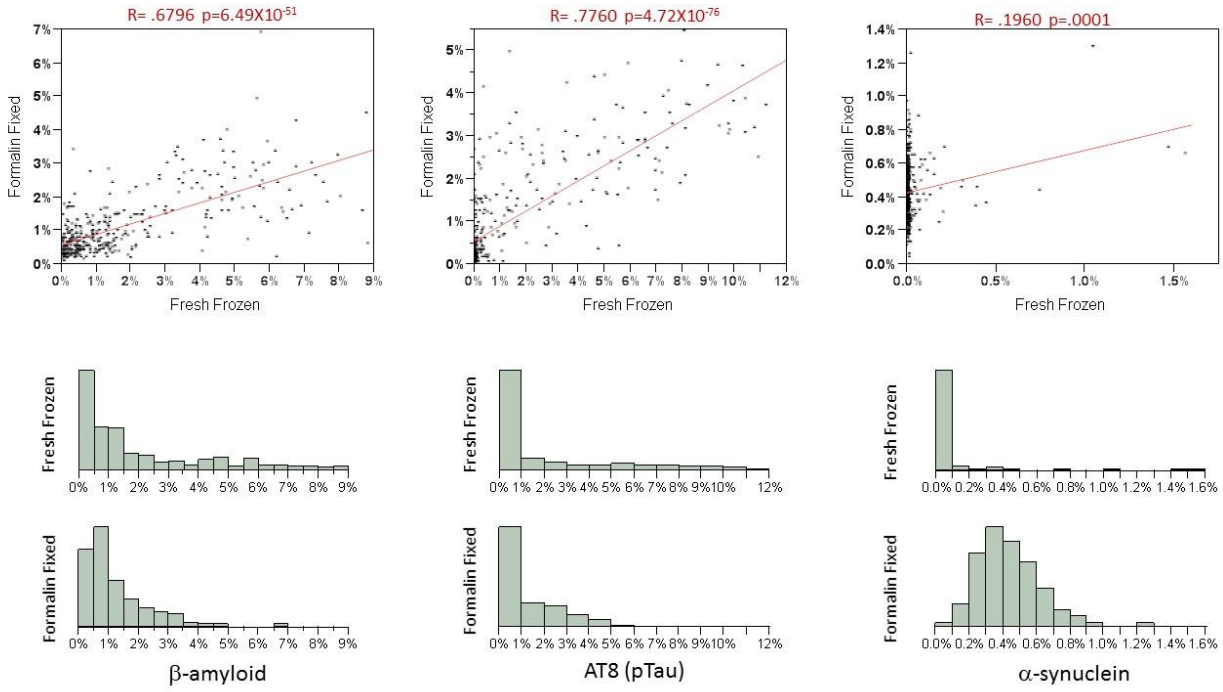

Figure 2. Correlation between IHC expression density metrics between fixed and fresh frozen tissue.
Top row: Good correlations were seen between quantifications of antibodies for β-amyloid and pTau in formalin-fixed (x-axes) and fresh frozen (y-axes) tissue, indicating good agreement between these two measures of pathology. In contrast, very low correlation was seen between quantifications for α-synuclein staining in formalin fixed vs. fresh frozen tissue. **Lower two rows:** scaled histograms showing the distribution of percent area covered by each pathology for fresh frozen (middle row) and formalin-fixed (bottom row) tissue. Five of the six distributions showed a one tailed distribution, indicating that a relatively small number of samples contained large amounts of pathology. The more Gaussian distribution of data points for the α-synuclein fixed tissue resulted from poor discrimination of signal and noise in cases with no pathology, which constituted the vast majority of tissue blocks, and therefore this metric was failed as unreliable.

PROTEIN QUANTIFICATION USING LUMINEX PLATFORM

Protein molecular changes in tau and phospho-tau variants, Aβ species, α-synuclein, inflammatory mediators (cytokines and chemokines), neurotrophic factors, and other targets were determined using multiplexed Luminex assays. Banked frozen tissues for TBI and control cases were identified that were immediately adjacent to those submitted for IHC, ISH, and RNA-Seq for parietal lobe, temporal lobe, and hippocampus. Tissue dissections are as described in the Tissue Collection Technical White Paper in Documentation. Tissues were processed through sequential extraction and centrifugation. In brief, tissues were homogenized by sonicating in 10 x volume of RAB buffer (0.1M 2-(N-morpholino) ethanesulfonic acid), 1mM ethylene glycol tetraacetic acid (EGTA), 0.5mM $MgSO_4$, 0.75M NaCl, 0.02M NaF, 1mM phenylmethylsulfonyl fluoride (PMSF), 0.1% protease inhibitor), and centrifuged (Optima TLX from Beckmann Coulter) at 36,000 rpm for 40 min at 4°C to clarify the homogenate. After supernatants were carefully collected and labelled as RAB extract, the resultant pellets were then re-homogenized in 5M guanidine-HCl or RIPA buffer (50mM Tris, 150mM NaCl, 1% Triton x-100, 5mM ethylenediaminetetraacetic acid (EDTA), 0.5% sodium deoxycholate, 0.1% lithium dodecyl sulfate, pH 8.0) and centrifuged at 36,000 rpm for 20 minutes at 4°C. Supernatants from the guanidine homogenates were collected and labelled as G extract, and supernatants from the RIPA homogenates were labelled as RIPA extract. The resultant pellets from RIPA homogenates were re-homogenized in 5M guanidine-HCl and centrifuged at 27,000 rpm for 20 minutes at 4°C. The collected supernatants were labelled as RG extract. All extracts were stored at -80°C until needed for Luminex assays.

Quantification of individual proteins was performed by using Luminex assay kits (singleplex bead kits or 11-plex custom bead kit) from Life Technologies. After preliminary assays to determinate the optimal extracts to be used for individual assays, RAB extracts were utilized to quantify BDNF (# LHC7071) and 11 plex-proteins (#

LHB0001CM). RIPA extracts were used for aggregated α-synuclein (# LHB0071). G extracts were used to quantify Ab40 (# LHB3481), Ab42 (# LHB3441), Tau (# LHB0041) and pT181-Tau (# LHB7051).

Luminex assays were performed according to the protocol provided by the manufacturer. In brief, 200 µl of Working Wash Solution (WWS) was added into each well of a 96-well filter plate (Millipore, # MSBVN1210) to pre-wet the plate, and the WWS was then aspirated using the vacuum manifold after incubation for 30 sec at room temperature. The diluted bead solution was vortexed for 30 sec and then sonicated for 30 sec. The diluted bead solution (25 µl) was added immediately into each well and the beads were washed twice with 200 µl of WWS. The filter plate was placed on clean paper towels to remove any residual liquid. Prepared 1x Detector Antibody (50 µl) was added into each well. Assay Diluent (25 µl) followed by 25 µl of sample was added to the sample wells, and 50 µl of appropriate standard dilutions were added to the standard curve wells. The plate was covered with aluminum foil to prevent exposure to light and incubated for 3 hrs at room temperature on an orbital shaker (500 rpm). After liquid was removed by aspiration with the vacuum manifold, beads were washed twice with 200 µl of WWS. R-Phycoerythrin (RPE) conjugate (100 µl of 1x RPE) was added to each well and the plate was incubated for 30 minutes at room temperature on an orbital shaker in the dark. Liquid was removed and beads were washed 3 times with 200 µl of WWS. Finally, 100µl of WWS was added to each well and the plate was incubated for 2 min on an orbital shaker. Fluorescence was analyzed using the LiquiChip Workstation (Qiagen).

The concentrations of samples were determined from the standard curve. Data were presented as picogram or nanogram of protein per milligram of tissue.

ISOPROSTANES

Free radical injury in parietal cortex and temporal cortex was determined using GC/MS quantitation of isoprostanoids. Isoprostane assays were conducted using the procedure detailed by Montine *et al*.[17] and Milatovic *et al*[18]. In summary, lipids were extracted using a modified Folch procedure, then saponified to release esterified prostanes. After addition of stable isotope-labeled internal standard, isoprostanes were isolated using reversed-phase and normal-phase solid phase extraction (SPE). Dried extracts were then derivatized to pentafluorbenzyl esters. Thin layer chromatography was used to remove excess reagent. Prior to GC/MS analysis, extracts were further derivatized to heat stable silyethers. GC/MS analysis was conducted using a 6890N Agilent gas chromatograph coupled to a 5973 quadrupole mass spectrometer in the negative-ion mode. Areas under peaks for *m/z* 569.5 and 573.2 (internal standard) were manually integrated to quantify both analyses.

REFERENCES

1. Hawrylycz, M.J. et al. An anatomically comprehensive atlas of the adult human brain transcriptome. *Nature* **489**, 391-9 (2012).
2. Miller, J.A. et al. Transcriptional landscape of the prenatal human brain. *Nature.* **508**, 199-206. doi: 10.1038/nature13185. Epub 2014 Apr 2. (2014).
3. Roth, R.B. et al. Gene expression analyses reveal molecular relationships among 20 regions of the human CNS. *Neurogenetics.* **7**, 67-80. Epub 2006 Mar 30. (2006).
4. Johnson, M.B. et al. Functional and evolutionary insights into human brain development through global transcriptome analysis. *Neuron.* **62**, 494-509. doi: 10.1016/j.neuron.2009.03.027. (2009).
5. Colantuoni, C. et al. Temporal dynamics and genetic control of transcription in the human prefrontal cortex. *Nature.* **478**, 519-23. doi: 10.1038/nature10524. (2011).
6. Kang, H.J. et al. Spatio-temporal transcriptome of the human brain. *Nature.* **478**, 483-9. doi: 10.1038/nature10523. (2011).
7. Blalock, E.M. et al. Incipient Alzheimer's disease: Microarray correlation analyses reveal major transcriptional and tumor suppressor responses. *Proc Natl Acad Sci U S A.* **101**, 2173-8. Epub 2004 Feb 9 doi:10.1073/pnas.0308512100. (2004).
8. Colangelo, V. et al. Gene expression profiling of 12633 genes in Alzheimer hippocampal CA1: transcription and neurotrophic factor down-regulation and up-regulation of apoptotic and pro-inflammatory signaling. *J Neurosci Res.* **70**, 462-73. (2002).

9. Miller, J.A., Woltjer, R.L., Goodenbour, J.M., Horvath, S. & Geschwind, D.H. Genes and pathways underlying regional and cell type changes in Alzheimer's disease. *Genome Med.* **5**, 48. doi: 10.1186/gm452. eCollection 2013. (2013).
10. Baker, S.C. et al. The External RNA Controls Consortium: a progress report. *Nat Methods.* **2**, 731-4. (2005).
11. Risso, D., Ngai, J., Speed, T.P. & Dudoit, S. Normalization of RNA-seq data using factor analysis of control genes or samples. *Nat Biotechnol.* **32**, 896-902. doi: 10.1038/nbt.2931. Epub 2014 Aug 24. (2014).
12. Aronesty, E. ea-utils: Command-line tools for processing biological sequencing data. (Expression Analysis, 2011).
13. Li, B., Ruotti, V., Stewart, R.M., Thomson, J.A. & Dewey, C.N. RNA-Seq gene expression estimation with read mapping uncertainty. *Bioinformatics.* **26**, 493-500. doi: 10.1093/bioinformatics/btp692. Epub 2009 Dec 18. (2010).
14. Langmead, B., Trapnell, C., Pop, M. & Salzberg, S.L. Ultrafast and memory-efficient alignment of short DNA sequences to the human genome. *Genome Biol.* **10**, R25. doi: 10.1186/gb-2009-10-3-r25. Epub 2009 Mar 4. (2009).
15. Miller, J.A. et al. Improving reliability and absolute quantification of human brain microarray data by filtering and scaling probes using RNA-Seq. *BMC Genomics.* **15**, 154 (2014).
16. Kadota, K., Nishiyama, T. & Shimizu, K. A normalization strategy for comparing tag count data. *Algorithms Mol Biol.* **7**, 5. doi: 10.1186/1748-7188-7-5. (2012).
17. Montine, T.J. et al. F2-isoprostanes in Alzheimer and other neurodegenerative diseases. *Antioxid Redox Signal.* **7**, 269-75. (2005).
18. Milatovic, D., VanRollins, M., Li, K., Montine, K.S. & Montine, T.J. Suppression of murine cerebral F2-isoprostanes and F4-neuroprostanes from excitotoxicity and innate immune response in vivo by alpha- or gamma-tocopherol. *J Chromatogr B Analyt Technol Biomed Life Sci.* **827**, 88-93. Epub 2005 Apr 19. (2005).